FABRICATION, CHARACTERIZATION AND FUNCTIONALITY OF $BaFe_{12}O_{19}$/EPOXY NANOCOMPOSITES

A. Sanida[1], S. G. Stavropoulos[1], Th. Speliotis[2] and G. C. Psarras[1]

[1] Smart Materials & Nanodielectrics Laboratory, Department of Materials Science, School of Natural Sciences, University of Patras, Patras 26504, Greece
ksanida@upatras.gr, http://www.smatlab.upatras.gr/
[2] Institute of Nanoscience and Nanotechnology, NCSR "Demokritos" Aghia Paraskevi, Athens 15310, Greece
t.speliotis@inn.demokritos.gr, http://www.ims.demokritos.gr/ims_field.php?ergo=G101

Keywords: Polymer nanocomposites, magnetic properties, dielectric response, thermomechanical behavior, barium ferrite

Abstract
In this study $BaFe_{12}O_{19}$/epoxy composite nanodielectrics were fabricated and studied. The morphological investigation was conducted by Scanning Electron Microscopy (SEM). The dielectric response was examined by means of Broadband Dielectric Spectroscopy (BDS). Thermomechanical characterization was carried out via Dynamic Mechanical Analysis (DMA) and Differential Scanning Calorimetry (DSC). Magnetic characterization was conducted by means of a Superconducting Quantum Interference Device (SQUID). The addition of the nanoparticles improves the dielectric and thermomechanical properties of the nanocomposites. Three different relaxation mechanisms were observed: Interfacial polarization, glass to rubber transition of the polymer matrix and re-orientation of polar side groups. The magnetic measurements confirmed the ferromagnetic nature of the nanocomposites.

1. Introduction

Nanocomposites based on ferrite-polymer mixtures constitute a wide active area of research, owing to their applications in electromagnetic interference shielding (EMI), drug delivery, drug targeting and as contrasting agents in magnetic resonance imaging (MRI) [1-3]. Magnetic nanocomposites possess unique physical and chemical properties compared to their bulk counter parts due to the constituents' nanodimension. Agglomeration, one of the main constrains in the synthesis of magnetic nanomaterials, can be removed by the use of a polymer matrix to isolate the particles [4-7].

M-type barium ferrite with hexagonal structure ($BaFe_{12}O_{19}$) is a well-known high-performance permanent magnetic material, because of its high magnetocrystalline anisotropy, high Curie temperature, relatively large magnetization, excellent chemical stability and corrosion resistance [8].

Specimens' morphology was assessed via SEM. The thermal properties were investigated by DSC and the mechanical characterization was conducted via DMA and static tensile tests, while dielectric and magnetic response were studied by means of BDS and magnetization measurements using SQUID, respectively.

2. Experimental

Nanocomposites were prepared by employing commercially available constituents. In particular, Epoxy resin and curing agent with trade names Epoxol 2004A and Epoxol 2004B, (both provided by Neotex S.A., Athens, Greece), while $BaFe_{12}O_{19}$ nanoparticles were obtained from Sigma-Aldrich, with diameter size less than 100 nm.

The preparation procedure involved mixing of the resin with the curing agent in a 2:1 (w/w) ratio and then adding various amounts of the nanoparticles. Filler's content was 1, 3, 5, 10, 15 20 phr (parts per hundred resin per mass). The mixture was stirred at a slow rate in a sonicator for 10 minutes. Subsequently, the mixture was poured into silicon molds and cured at ambient for 7 days. The post curing took place for 4 hours at 100^{o}C. The morphology of the produced specimens was checked for the presence of clusters, while the quality of the filler dispersion within the polymer matrix was examined via SEM (EVO MA 10, ZEISS).

The thermal and dynamic mechanical investigation were carried out via Differential Scanning Calorimetry (DSC), in the temperature range from 20^{o}C to 100^{o}C with 5^{o}C/min heating rate and Dynamic Mechanical Analysis (DMA) in the temperature range from room temperature to 100^{o}C with 5^{o}C/min heating rate, using TA Q200, TA Q800 devices respectively, both provided by TA Instruments. For the DSC tests, samples were placed in an aluminum crucible, while an empty aluminum crucible was serving as reference. The DMA experiments were conducted in the three-point bending configuration using suitable rectangular shaped specimens at f=1 Hz. Additionally, the mechanical properties of nanocomposites were examined with static tensile tests using an Instron 5582 apparatus provided by Instron, at room temperature with 5mm/min tension rate.

The dielectric response of the nanocomposites was studied by means of Broadband Dielectric Spectroscopy using an Alpha-N Frequency Response Analyzer, while a Novotherm system was used for the temperature control; both devices were supplied by Novocontrol Technologies. Experimental data were obtained automatically via suitable software (Windeta), by performing isothermal frequency scans. The applied frequency range for the nanocomposites was 10^{-1}-10^6 Hz from 30 to 160 ^{o}C, with a temperature step of 10 ^{o}C, employing the dielectric cell BDS 1200 respectively. The amplitude of the time varying voltage was equal to 1V in all cases. Dielectric cell and software were also supplied by Novocontrol Technologies. The magnetic characterization was conducted by employing a Superconducting Quantum Interference Device (SQUID) magnetometer, supplied by Quantum Design. The maximum applied magnetic field was 50 kOe.

3. Results and Discussion

3.1. Morphological characterization

Fig. 1a, and b depicts representative SEM images for the 1 and 15 phr $BaFe_{12}O_{19}$/epoxy nanocomposites revealing that fine nanodispersion of ceramic particles has been achieved, with limited or even no agglomeration.

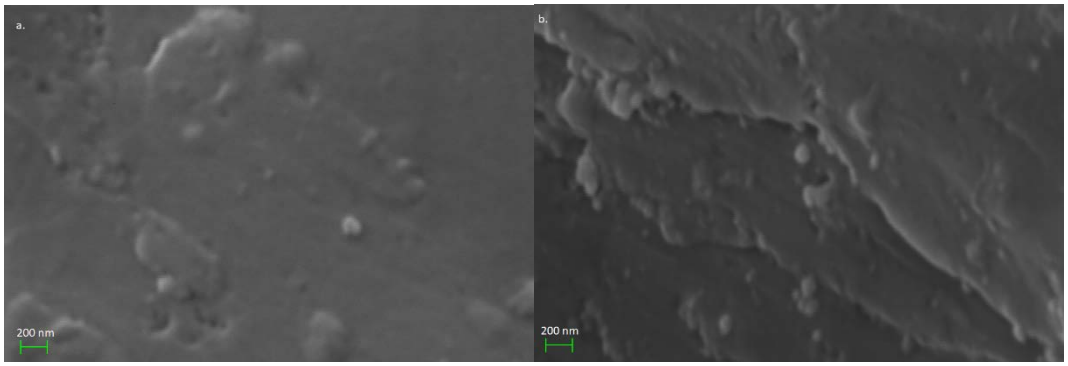

Figure 1. SEM images for the nanocomposites with: (a) 5 phr, (b) 20 phr in $BaFe_{12}O_{19}$ content**.**

3.2. Thermomechanical Characterization

The glass transition temperature acquired via BDS, DMA and DSC experiments are presented in Table 1, for all examined systems. An endothermic step-like transition was identified in the DSC thermograms of all examined systems, which is attributed to the glass to rubber transition of the polymer matrix. The glass transition temperatures (T_g) were determined using the point of inflection of the transition via suitable software, provided by TA Instruments. All $BaFe_{12}O_{19}$ nanocomposites exhibited lower T_g than the polymer matrix. The DSC results gave a different image, probably because of the localized nature of this technique, as it examines a very small sample from a specific area of the nanocomposite, and the dynamic nature of the glass to rubber transition.

In the spectra of all specimens, a step-like decrease of storage modulus is observed at 45 to 70 ^oC indicating the presence of α-relaxation process, which is attributed to the glass to rubber transition of the polymer matrix. The glass transition temperature of each system was determined by the peak of the loss modulus diagram and the obtained values are also listed in Table 1.

Glass transition temperature ($T_{g,diel}$) can also be estimated via dielectric data, by employing the convention that τ ($T_{g,diel}$) = 100 s, which relates the relaxation time (τ) of α-mode with T_g [4], [9].

Variation of T_g implies the predominat interactions, between macromolecules/particles, or particles/particles. Increase of T_g denotes strong interactions between polymer and particles, while decrease of T_g signifies the particle/particle interactions as the prevalent ones.

Table 1. Glass transition temperatures and mechanical properties for all examined systems.

Specimens	**DSC**	**DMA**	**BDS**	**Tensile Tests**	
	T_g (^oC)	T_g (^oC)	T_g (^oC)	*Young's Modulus* (MPa)	*Tensile Strength* (MPa)
Epoxy	50.1	50.6	47.9	1865	29.504
1 phr	48.7	51.2	47.6	2044	29.782
3 phr	48.1	50.9	45.0	2003	29.987
5 phr	48.6	54.7	42.4	2372	29.976
10 phr	48.1	52.4	37.3	2351	26.430
15 phr	48.6	52.6	42.7	2464	24.834
20 phr	48.8	52.9	43.2	2688	21.220

The mechanical properties of the fabricated nanocomposites were tested using an Instron 5582 tensile tester. The addition of nanoparticles seems to improve the mechanical properties of all examined systems, as shown in Table 1, where the Young's modulus is depicted. The $BaFe_{12}O_{19}$ systems exhibit a gradual, in three-steps, increase of Young's modulus values, at low (1 and 3 phr), intermediate (5, 10, 15 phr) and high concentration (20 phr), respectively. The tensile modulus was calculated as the slope of the stress/strain curve in the elastic region. Data analysis demonstrates a substantial increase of the Young's modulus (2.68 GPa), of up to 44% for the 20 phr reinforced specimen, compared to the unfilled matrix (1.86 GPa). The increment of tensile modulus is attributed to the reinforcing ability and rigidness of the ceramic nanoparticles and to the strong interfacial bonding between the matrix and the nanoinclusions.

3.3. Dielectric Characterization

The variation of the real part of dielectric permittivity and loss tangent as a function of temperature and frequency is displayed in Figs. 2, for the 15 phr reinforced sample.

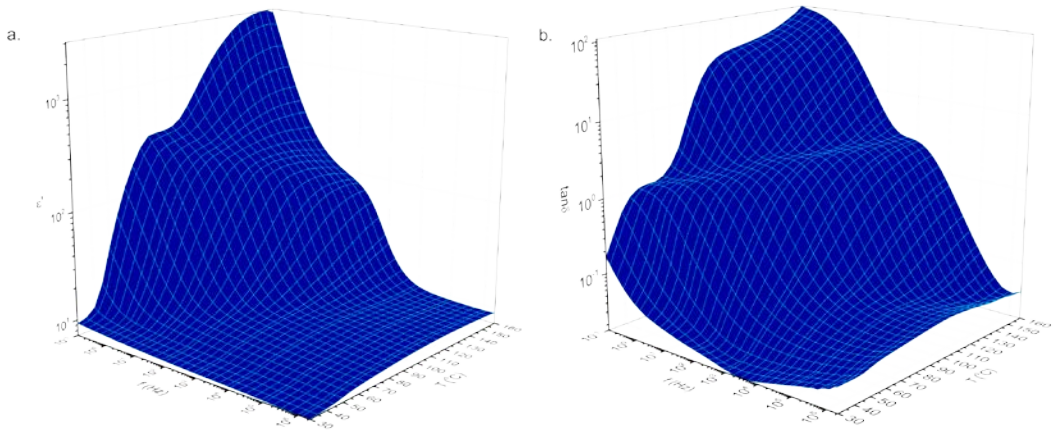

Figure 2. (a) Real part of dielectric permittivity and (b) loss tangent as a function of temperature and frequency for the nanocomposite with 15 phr in $BaFe_{12}O_{19}$ content.

Permittivity increases with diminishing of frequency, since dipoles attain sufficient time to orient themselves in the direction of the alternating field, while with the increase of frequency dipoles are no longer able to follow the alternation of the field. In the plot of loss tangent versus temperature and frequency (Fig. 2b) three different relaxation mechanisms were recorded. These are attributed to both the polymer matrix and the ceramic nanoinclusions. MWS effect is observed at low frequencies and high temperatures due to the heterogeneity of the systems, which favors the development of charges at the systems' interface. α-relaxation ascribed to glass to rubber transition of the polymer matrix, is recorded at intermediate frequencies, and β-relaxation due to the re-orientation of small polar side groups of the main polymer chain at high frequencies.

The variation of the real part of dielectric permittivity as a function of frequency is depicted in Fig. 3a, for all the examined system, at 40 °C.

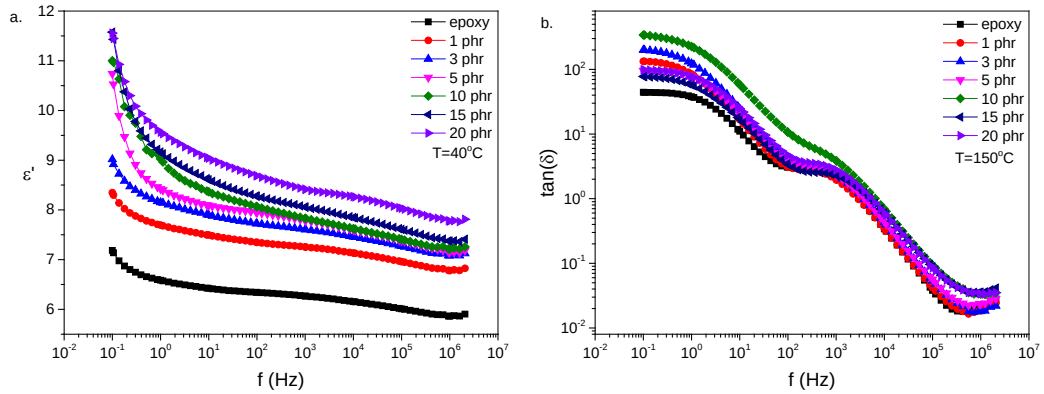

Figure 3. (a) Real part of dielectric permittivity and (b) loss tangent as a function of frequency, for all the examined systems, at 40 ºC and 150 ºC, respectively.

As expected, ε' increases with filler content in the whole frequency range, since barium ferrite nanoparticles exhibit higher values of permittivity than the polymer matrix. Comparative plots of the loss tangent (tan δ), as a function of frequency, for all the examined specimens, at 150 °C, are shown in Fig. 3b. The previously mentioned relaxations are present in these loss spectra. Until the 10 phr specimen the values of loss tangent was increasing with concentration and then diminish. This should be related to the high values of the dielectric loss, since tanδ is defined as the ratio of the imaginary to the real part of dielectric permittivity and further increase of the content reflect the increase of ε'' due to the enhanced heterogeneity.

The variation of the real and imaginary part of the electric modulus index as a function of frequency at 40 and 150 ºC, for the examined systems is depicted in Fig. 4, respectivly. As it can be seen (M′) decreases with $BaFe_{12}O_{19}$, as a result of the increase in the real part of permittivity. The recorded loss peaks in (M″) are associated with α-relaxation process. Relaxation peaks move towards higher frequencies as temperature increases and at the same time their maximum diminishes as the filler content increases, at constant temperature.

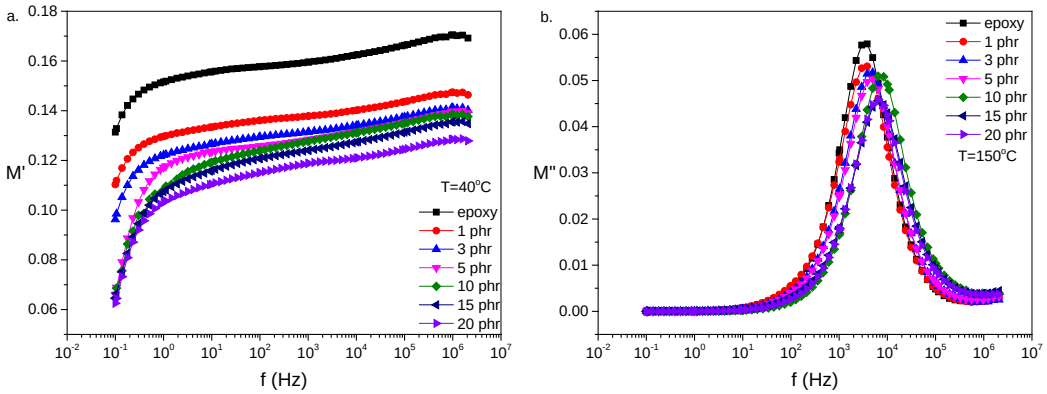

Figure 4. (a) Real part and (b) Imaginary part of electric modulus as a function of temperature, for all the examined systems, at 40 ºC and 150 ºC, respectively.

Dielectric Reinforcing Function (DRF) is defined [10] as follows:

$$G\ (\omega)|_T = \frac{\acute{\varepsilon}_{comp}(T)}{\acute{\varepsilon}_{mat}\ (T)} \quad (1)$$

Fig. 5 shows the variation of DRF with frequency. DRF can be considered as a measure of the acquired normalized polarization, expressing the dielectric reinforcing efficiency of the employed filler and the achieved level of energy storing.

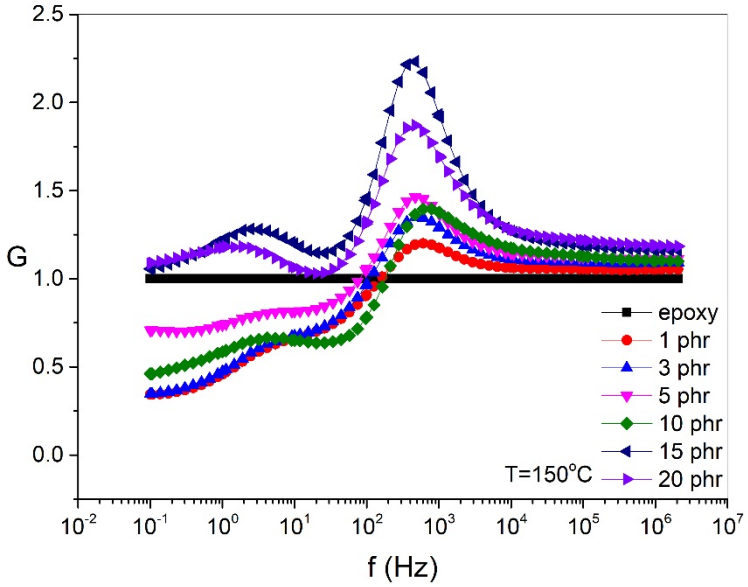

Figure 5. DRF as a function of frequency, for all the examined systems, at 150 °C.

Values of G(ω, T) function are normalized with respect to polymer matrix and thus reflect only the fillers contribution as well as possible interactions between ceramic inclusions and polymer matrix. In general, the ability of the nanocomposites for energy storage increases with barium ferrite content, and exceeds by more than 2 times the neat epoxy matrix, at the maximum point of the function. The relative energy density function varies with the ratio of composites' real part of dielectric permittivity upon the corresponding one of the matrix, expressing the normalized polarization of the systems. Thus, the occurring peaks in their spectra are related to polarization effects occurring in the under examination nanocomposites. The peak formed at intermediate frequencies is attributed to the α-relaxation process and its position could be affected by the variation of dynamics of the α-process, between the polymer matrix and the nanocomposites. The weaker peaks appearing as fluctuations in the lower frequencies range correspond to interfacial polarization due to the accumulation of free charges at the interface between the filler and the polymer matrix.

3.4. Magnetic Characterization

Representative magnetization hysteresis curves for barium ferrite nanopowder and $BaFe_{12}O_{19}$/epoxy nanocomposites are depicted in Fig. 6. Neat barium ferrite exhibits the highest values of magnetization and coercivity, Fig. 6 inset (uper left). Additionally, nanocomposites' magnetization and coercivity increases systematically with filler content, as expected, Fig. 6. The room temperature magnetization hysteresis behaviour of the samples shows a clear magnetic hysteresis behaviour with coercivity of 1330 Oe and the saturation magnetization (M_s) value increases with filler content.

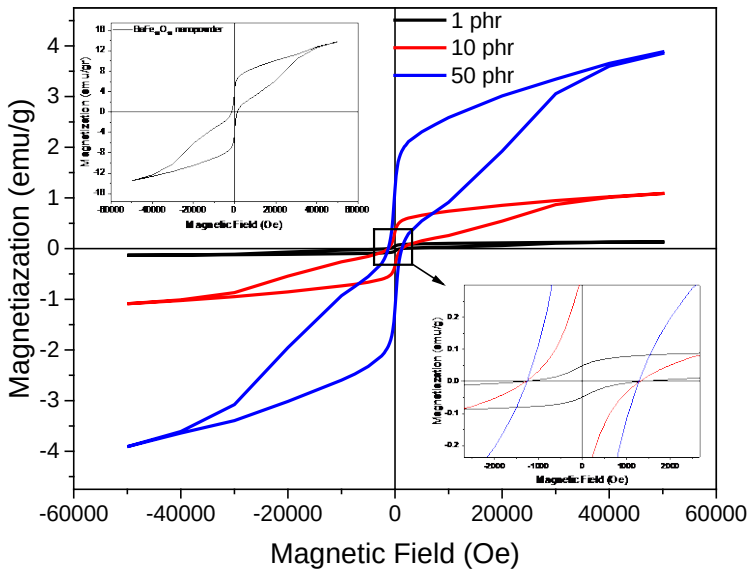

Figure 6. Magnetic hysteresis loops for the nanocomposites with 1, 10, 15 phr $BaFe_{12}O_{19}$ content, at 30 °C. Inset (above) depicts the magnetic hysteresis loop of $BaFe_{12}O_{19}$ nanopowder, at 30 °C. Inset (below) demonstrate the coercive field of the nanocomposites.

4. Conclusions

A series of nanocomposites consisting of epoxy resin and $BaFe_{12}O_{19}$ nanoparticles were successfully fabricated and characterized morphologically via scanning electron microscopy. Their thermal properties were studied via differential scanning calorimetry and the mechanical properties using dynamic mechanical analysis and static tensile tests and their dielectric response was investigated by means of broadband dielectric spectroscopy. Finally, the magnetic behaviour was derived from data obtained by superconducting quantum interference device. From the experimental data, it seems that the incorporation of the ceramic nanoparticles enhances significantly both the mechanical and the dielectric properties of the examined systems. Three distinct relaxation mechanisms were recorded in the spectra of all systems and were attributed to the polymer matrix and the filler inclusions: Interfacial polarization, also known as Maxwell-Wagner-Sillars phenomenon is observed at low frequencies and high temperatures due to the heterogeneity of the systems, α-relaxation is ascribed to glass to rubber transition of the matrix, at intermediate frequencies, and β-relaxation due to the re-orientation of small polar side groups of the polymer chain at high frequencies. The magnetic measurements confirmed the ferromagnetic nature of the nanocomposites. The induced magnetic properties increase with the inclusion of hexaferrite nanoparticles.

Acknowledgements

This research has been financially supported by the General Secretariat for Research and Technology (GSRT) and the Hellenic Foundation for Research and Innovation (HFRI) (Scholarship Code: 10566).

References

[1] L. S. Schadler, L. C. Brinson, and W. G. Sawyer. Polymer nanocomposites: A small part of the story. *Jom*, 59:3:53–60, 2007.
[2] F. Hussain. Review article: Polymer-matrix Nanocomposites, Processing, Manufacturing, and

Application: An Overview. *Journal of Composite Materials*, 40:17:1511–1575, 2006.
[3] T. Hanemann and D. V. Szabó. Polymer-Nanoparticle Composites: From Synthesis to Modern Applications. *Materials*, 3:6:3468–3517, 2010.
[4] A. Sanida, S. G. Stavropoulos, T. Speliotis, and G. C. Psarras. Development , characterization , energy storage and interface dielectric properties in $SrFe_{12}O_{19}$ / epoxy nanocomposites. *Polymer*, 120:73–81, 2017.
[5] S. Sindhu, S. Jegadesan, A. Parthiban, and S. Valiyaveettil. Synthesis and characterization of ferrite nanocomposite spheres from hydroxylated polymers. *Journal of Magnetism and Magnetic Materials*, 296:2:104–113, 2006.
[6] G. C. Psarras, Smart polymer systems: A journey from imagination to applications. *Express Polymer Letters*, 5:12:1027, 2011.
[7] A. Sanida, S. G. Stavropoulos, T. Speliotis, and G. C. Psarras. Development , multiple characterization and functionality in magnetic nanoparticles – polymer matrix nanodielectrics. *Materials Today: Proccedings.* (in press)
[8] C. Tsonos, N. Soin, G. Tomara, B. Yang, G. C. Psarras, A. Kanapitsas, and E. Siores. Electromagnetic wave absorption properties of ternary poly(vinylidene fluoride)/magnetite nanocomposites with carbon nanotubes and graphene. *RSC Advances*, 6:3:1919–1924, 2016.
[9] A. Vassilikou-Dova and M. Kalogeras, *Dielectric Analysis (DEA)* in *Thermal Analysis of Polymers*. John Wiley & Sons, Inc., 497-613, 2009.
[10] G. Ioannou, A. Patsidis, and G. C. Psarras. Dielectric and functional properties of polymer matrix/ZnO/$BaTiO_3$ hybrid composites. *Composites Part A: Applied Science and Manufacturing*, 42:1:104–110, 2011.